Journal of Zhejiang University-SCIENCE A (Applied Physics & Engineering)
ISSN 1673-565X (Print); ISSN 1862-1775 (Online)
www.jzus.zju.edu.cn; www.springerlink.com
E-mail: jzus@zju.edu.cn

Numerical study on cavity ignition process in a supersonic combustor*

Yong-chao SUN[1], Zun CAI[†‡1], Tai-yu WANG[1], Ming-bo SUN[1], Cheng GONG[2], Yu-hui HUANG[1]

[1]*Science and Technology on Scramjet Laboratory, College of Aerospace Science and Engineering, National University of Defense Technology, Changsha 410073, China*

[2]*China Aerodynamics Research and Development Center, Mianyang 621000, China*

[†]E-mail: caizun1666@163.com

Received Aug. 24, 2019; Revision accepted Feb. 13, 2020; Crosschecked July 15, 2020

Abstract: Large eddy simulations (LESs) of cavity ignition processes were performed in a 2D ethylene-fueled supersonic combustor with a single rear-wall-expansion cavity based on OpenFOAM. The ethylene combustion was modelled using a 35-step with 20-specie ethylene chemical mechanism, which had been validated by CHEMKIN calculations. The effect on the ignition process of different ignition sites inside the cavity was then studied. It was found that the rear region of the cavity floor is an optimized ignition site where successful ignitions will be achieved. According to different ignition behaviors, two flame extinguishing modes could be identified: blown-off extinguishing mode and flow dissipation extinguishing mode. Blown-off extinguishing mode mainly occurred after ignition near the cavity shear layer, in which the initial flame was blown off directly due to the high speed of the supersonic core flow. Flow dissipation extinguishing mode is likely to occur after ignition near the front and middle cavity floor as a result of severe turbulent dissipations and limited chemical reactions. The study indicates that the movement routine of the initial flame is important for the ignition process, including both moving towards a favorable flow field and forming a large heat release region along the movement.

Key words: Ignition process; Cavity; Supersonic combustor; Numerical study
https://doi.org/10.1631/jzus.A1900419 **CLC number:** V43

1 Introduction

The scramjet propulsion system is currently the most promising air-breathing propulsion technology for commercial flight and space access (Curran, 2001; Huang et al., 2016; Lv et al., 2017; Chang et al., 2018). To achieve a successful ignition and a stabilized flame in a supersonic flow, cavity-based flame holders are widely used in the scramjet combustor (Ben-Yakar and Hanson, 2001; Mathur et al., 2001; Huang and Yan, 2013; Huang et al., 2013). The cavity-based flame holders are more effective in a real scramjet combustor with fuel injectors integrated into the flame holders (Sun et al., 2012). In the past decades, cavity-stabilized ignition and combustion have been widely investigated (Wang et al., 2014; Barnes and Segal, 2015).

Due to the harsh supersonic flow and limited chemical reaction environment, successful ignition processes are still difficult to achieve even with a cavity flame holder. To make it easier to investigate the simulation of cavity ignition and flame stabilization in real scramjet applications, ethylene is often used as fuel in a model cavity-based supersonic combustor as the C/H ratio of ethylene is very close to

‡ Corresponding author
* Project supported by the National Natural Science Foundation of China (Nos. 11902353 and 51706238) and the Postdoctoral Innovation Talent Support Program of China (No. BX20190091)
ORCID: Yong-chao SUN, https://orcid.org/0000-0002-1825-9032

that of kerosene. Potturi and Edwards (2015) applied a hybrid large eddy simulation/Reynolds-averaged Navier–Stokes (LES/RANS) method to investigate ethylene combustion in a cavity flame holder using a 22-specie chemical mechanism. It appeared that the flame propagated into a stoichiometric to fuel-rich mixture near the cavity according to the analysis of the flame structure predicted by the LES/RANS method. In addition, both the premixed and non-premixed flames existed in the combustion process (Potturi and Edwards, 2015). Wang et al. (2015) conducted RANS with a shear stress transport (SST) k-ω turbulence model to investigate the combustion process based on a classical three-step ethylene chemical mechanism. They found that fuel/air mixing and combustion occurred mainly in the vicinity of the bottom wall of the combustor due to fuel injection on that wall. Besides, high non-symmetry in the distributions of the bottom and the top wall heat fluxes was observed (Wang et al., 2015). Li et al. (2015) studied the ethylene ignition transient assisted by air throttling numerically by using a two-step global chemical mechanism. In their study, air throttling was activated once fuel injection was steady and the spark plug was on, then air throttling was removed immediately after flame stabilization was achieved. They found that a shock train was generated in the isolator as a consequence of back pressurization by the throttling air, which decelerated the high-speed in the supersonic core flow, enhanced the fuel/oxidizer mixing, and increased the temperature and pressure in the combustor (Li et al., 2007; Yang et al., 2010).

In the open literature, the flame stabilization process inside an ethylene-fueled cavity has been widely emphasized, while the ignition process has been less focused upon and has been investigated with a less accurate chemical mechanism. Furthermore, flame extinction during the ignition process and its mechanism are rarely mentioned. To ensure successful ignition processes, both flame growing and extinguishing mechanisms should be comprehensively understood. In this study, 2D ethylene ignition processes inside a rear-wall-expansion cavity based on a 35-step with 20-specie chemical mechanism are conducted by LES. The effect of the ignition site on the ignition process is discussed. Mechanisms regarding flame growing and extinguishing processes are emphasized.

2 Model and numerical method

2.1 Boundary conditions

Since the initial flame behaviors mainly occur in the stream-wise direction and to reduce the computational cost, a 2D simulation is sufficient and is applied in this study. A schematic of the 2D computational domain investigated in this study is given in Fig. 1. The supersonic combustor is made up of an isolator, a rear-wall-expansion cavity, and an expansion section. The isolator is applied to constrain the interaction between the shock-wave trains and the inflow during the combustion process. The expansion section is an extended part of the combustor, and is used to improve combustion in the combustor and to generate thrust for the scramjet engine.

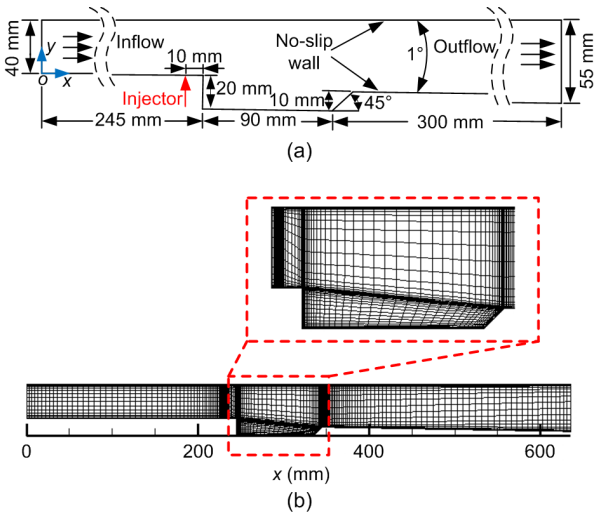

Fig. 1 Combustor and grid for the simulations: (a) schematic of the supersonic combustor; (b) grid used for the simulations

As depicted in Fig. 1a, the front wall depth, rear wall depth, cavity floor length, and aft ramp angle of the cavity are 20 mm, 10 mm, 90 mm, and 45°, respectively. As the rear wall depth is lower than the front wall depth, the cavity geometry is referred to a rear-wall-expansion cavity. The bottom wall of the combustor has an expansion angle of 1°. There is an injection slot located at 10 mm upstream the cavity with a width of 0.25 mm. Pure ethylene is used as fuel and is injected through the injection slot.

In the computational domain, adiabatic and non-slip boundary conditions are applied to the top

and bottom walls. Pressure inlet conditions are applied at the inlet of the combustor and the injection slot, where static pressure and static temperature are specified. In the span-wise direction (z), the periodic condition is used. The inflow conditions as well as the injection conditions are set according to the experimental related parameters (Cai et al., 2018a), as listed in Table 1.

Table 1 Boundary conditions for the computational domain

Parameter	Value	
	Inflow	Fuel
Total temperature (K)	1530	300
Total pressure (MPa)	2.6	1.5
Mach number, Ma	2.92	1.0
Y_{O_2} (%)	23.3	0.0
Y_{H_2O} (%)	5.9	0.0
Y_{CO_2} (%)	9.6	0.0
Y_{N_2} (%)	61.2	0.0
$Y_{C_2H_4}$ (%)	0.0	100.0
Equivalence ratio, ϕ	0.30	0.30
Characteristic length, l (m)	0.635	0.635
Reynolds number, Re	5.7×10^7	5.7×10^7

Y indicates the specie mass fraction

2.2 Grid generation

To better solve the flow field, uniform structured grids are generated by Gridgen. Most typical flow field characteristics such as shock waves, vortex structures, and boundary layers are captured well by the grid. The grids are clustered towards the top and bottom walls of the combustor as well as the injection slot and are relaxed towards the inlet and outlet. The height of the first cell is 0.01 mm inside both the top and bottom walls of the combustor, leading to a favorable value of y+ of the grid. A grid with 134 167 cells is employed in the present study, and y+ is 1–40. The grid used for simulations is shown in Fig. 1b. To clearly show the grid, the total cell number shown in Fig. 1b is 27 000, which is less than that used for simulations.

2.3 Numerical methods

In this study, the LES method is applied for all the ignition cases. One-equation eddy model is used to solve the unclosed sub-grid terms in the Navier–Stokes equations. The partially stirred reactor (PaSR) model is used as the chemical reaction model. For detailed descriptions of the LES equations as well as the chemical reaction model, please refer to Cai et al. (2016, 2018b) and Wang et al. (2016).

An open-source computational fluid dynamics (CFD) library OpenFOAM is used in this study, which is based on finite volume methods. The numerical solver used is an improved version based on a density-based fully compressible flow solver, which is suitable for solving multi-specie non-reaction and reacting supersonic issues. The convective terms are discrete by using the second-order Kurganov and Tadmor approach with the van Leer limiter. The temporal terms are discrete by using the second-order backward Euler scheme. The Courant-Friedrichs-Lewy (CFL) number used in this study is about 0.2 leading to a physical time step of 1×10^{-8} s. Each case is run for 10 flow-through times.

3 Results and discussion

In this section, the ethylene chemical mechanism used in this study is first validated against available experimental data to make sure that the present mechanism is favorable for the ignition simulation. As the numerical solver has been proved to be suitable for simulating the supersonic combustion process by many related validations (Cai et al., 2016, 2017, 2018a, 2018b, 2018d; Wang et al., 2016), the validation of the numerical solver is ignored here. However, the combustion processes regarding different ignition sites will be discussed comprehensively.

3.1 Validation

Because its C/H ratio is very close to that of kerosene, ethylene is widely used in supersonic combustion simulations. In the open literature, many ethylene chemical mechanisms have been reported ranging from detailed (hundred steps) to reduced (three steps or even global) mechanisms. In this study, the three most widely used mechanisms were selected to validate 0D and 1D flame calculations in CHEMKIN and Cantera. These mechanisms are referred to as 35-step with 20-specie (Dong et al., 2008), 10-step with 10-specie (Baurle et al., 1998),

and 3-step with 7-specie (Baurle et al., 1998) mechanisms. Laminar flame burning velocity, adiabatic temperature, and ignition delay time and process are the most typical combustion characteristics and are often selected as key comparison parameters for chemical kinetic mechanism validations. Fig. 2 presents the comparative results of the calculations for the above three mechanisms with the available experimental data (Egolfopoulos and Law, 1991; Hassan et al., 1998; Jomaas et al., 2005; Kumar et al., 2008; Liu et al., 2017) and mechanism of University of Southern California (USC), the USA (Wang et al., 2007).

Laminar flame velocity is calculated in Fig. 2a at 298 K and 1 atm (1 atm=101 325 Pa). It is observed that the laminar flame velocity of the 35-step mechanism at different equivalence ratios shows a good agreement with the experimental data and USC. However, the 10-step and 3-step mechanisms obviously under-predict the experimental data and even present wrong variation tendencies. For the adiabatic temperature in Fig. 2b, it is seen that all the mechanisms present a similar tendency and the 35-step mechanism matches the USC quite well at an equivalence ratio larger than 1.5.

The ignition delay time is calculated at both different temperatures and different pressures as shown in Fig. 2c. It is found that, because of their consideration of the intermediate species, both the 35-step and 10-step mechanisms could well predict the ignition delay time. The ignition process is also validated by comparing the 35-step mechanism with the USC as depicted in Fig. 2d. Although the ignition process is a little slower using the 35-step mechanism, it only causes minor differences in the variation tendency. Therefore, taking the computational cost and accuracy into consideration, the 35-step mechanism is most suitable for the simulation of ethylene supersonic combustion, especially for the case of ignition transience and initial flame spreading.

3.2 Ignition process simulations

In this study, ignition process will be emphasized numerically by comparing different ignition sites inside the cavity. The ignition method is to patch a square region (5 mm×5 mm) with a local high temperature of 2000 K in the steady non-reaction flow field, and then calculate the unsteady reacting flow field. It should be noted that the patch location is

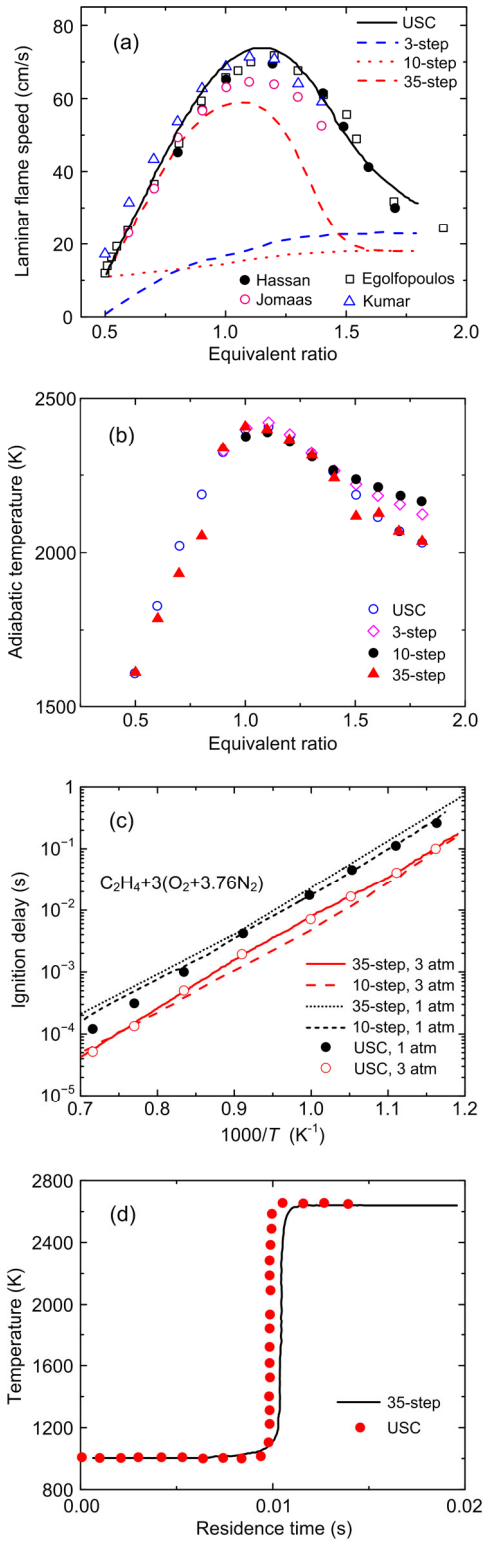

Fig. 2 Comparisons of different mechanisms with experimental data (Egolfopoulos and Law, 1991; Hassan et al., 1998; Jomaas et al., 2005; Wang et al., 2007; Kumar et al., 2008): (a) laminar flame speed; (b) adiabatic temperature; (c) ignition delay; (d) ignition process

related to the experimental setup (Cai et al., 2018a, 2018c), while the size of the square region is approximately equal to that of the spark (Cai et al., 2018e). In addition, it is also revealed that a square region with a high temperature of 2000 K (Cai et al., 2017) is favorable for the simulation of the ignition process.

There are four simulation cases conducted in this study, with the only difference being the ignition site as depicted in Fig. 3. Inside the cavity, there are three ignition sites located in the front, middle, and rear of the cavity, respectively. Outside the cavity, there is an ignition site located in the rear shear layer region. The detailed locations of these ignition sites are depicted clearly in Fig. 3.

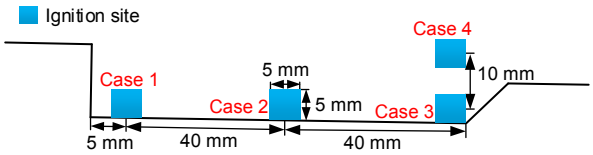

Fig. 3 Schematic of the ignition sites

The heat release rate (HRR) and H_2O distributions in the local cavity region during the ignition process of case 1 are shown in Fig. 4. The HRR distribution can be used to indicate the chemical reaction region and the flame, while the H_2O distribution can be used to indicate the hot combustion product. It can be seen that chemical reactions around the patch region in the front cavity are initiated at 0.2 ms after the ignition moment (t_0); that can be defined as the initial flame. This initial flame then propagates upstream towards the cavity leading edge and causes chemical reactions both in the jet wake region between the fuel jet and the cavity leading edge and in the left corner region on the cavity floor. Finally, the initial flame extinguishes gradually in the left corner region on the cavity floor. A flame extinguishing process is shown in Fig. 4 after ignition in the front region inside the cavity. In Fig. 5, the HRR distribution of the case 2 at t_0+1.8 ms is similar with that at t_0+0.6 ms in case 1; the H_2O evolution of the case 2 after t_0+1.8 ms is similar with that after t_0+0.6 ms in case 1. This indicates that the mechanisms of the extinguishing process in cases 1 and 2 are similar.

To further investigate the mechanism of the extinguishing process in case 1, the temperature distribution and the streamlines for it are shown in Fig. 6. R_1 and R_2 in Fig. 6 indicate the different directions of the flow stream. R_2 shows the region at which the flow stream moves toward the shear layer, while R_1 shows the region where the flow stream moves upstream of the cavity. Due to the evolution of the flow stream, the high temperature region can be observed at the upstream of the cavity, and it can also be observed at the shear layer.

The green color in regions T_1 and T_2 indicates that the temperature in these regions is higher compared with that at t_0+0.2 ms. The high temperatures in regions T_1 and T_2 are caused by the flow stream moving towards the shear layer as mentioned above. The distribution of the shear layer in this combustor had already been shown by Cai et al. (2016). The shear layer located in the rear cavity can also be observed in previous study (Zhao et al., 2016). The

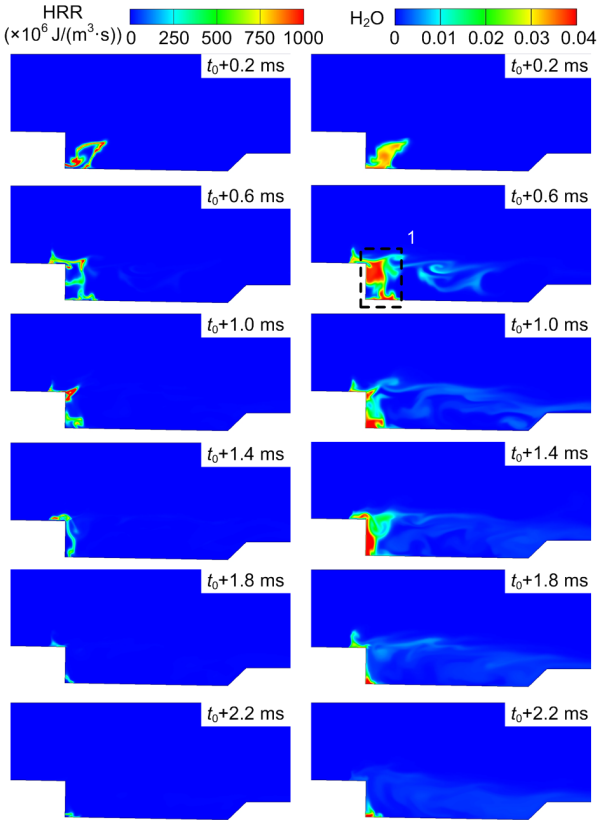

Fig. 4 Dissipation extinguishing mode after ignition in the front of the cavity floor (case 1). References to color refer to the online version of this figure

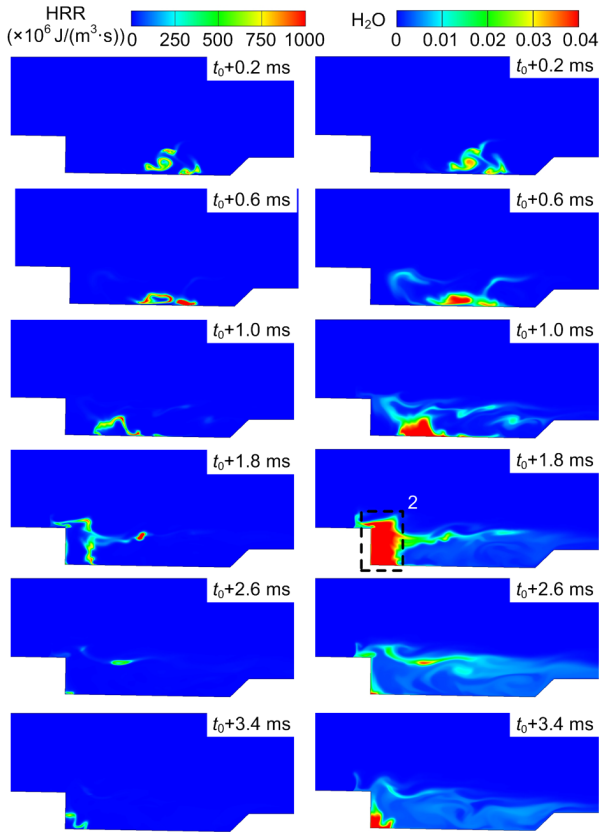

Fig. 5 Dissipation extinguishing mode after ignition in the middle of the cavity floor (case 2). References to color refer to the online version of this figure

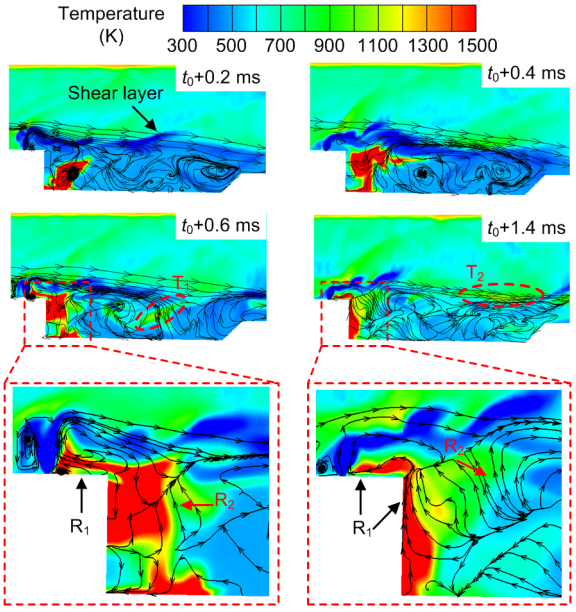

Fig. 6 Evolution of the high temperature region (case 1). References to color refer to the online version of this figure

high temperature stream moves out of the cavity due to the evolution of the flow stream, which further induces a decrease in the area of the high temperature region at t_0+1.4 ms. The combustion process cannot be sustained due to the decreasing area of the high temperature region. This reveals the mechanism of the extinguishing phenomenon in case 1. As discussed in Figs. 4 and 5, the mechanisms of the extinguishing process in cases 1 and 2 are similar.

From the discussions mentioned above, it can be concluded that the ignition energy in the high temperature region in cases 1 and 2 is dissipated by the flow stream evolution. In this study, the extinguishing mode in cases 1 and 2 is described as the flow dissipation extinguishing mode. The flow dissipation extinguishing mode means the extinguishing process is caused by the ignition energy dissipation dominated by the flow stream evolution.

Fig. 5 depicts similar HRR and H_2O distribution variations in the local cavity region of case 2 as in case 1. After ignition in the middle of the cavity floor, the initial flame still undergoes an extinguishing process which can also be classified as dissipation extinguishing mode. Compared with case 1, case 2 takes a longer time to achieve the final state of weakened flame located in the left corner on the cavity floor, and the flame is stronger than that of case 1 at the same time. It can be observed from Figs. 4 and 5 that the mass fraction of H_2O in zone 2 is greater than that in zone 1. For all the cases in this study, the boundary conditions of the inflow and fuel injection were kept the same. As a result, there is no difference in the fuel mass fraction distribution before ignition. The greater mass fraction of H_2O in zone 2 indicates the fuel in zone 2 is consumed more than that in zone 1. Consuming more fuel in zone 2 forms a larger heat release region, which leads to a stronger flame and a longer flame extinguishing process.

Based on the discussion on Figs. 4 and 5, it can be concluded that forming a larger heat release region is beneficial for the ignition process. Generally, there are two ways to increase the heat release region by consuming more fuel during the ignition process, either by increasing the local fuel mass fraction or increasing the initial flame movement towards the cavity angular recirculation zone where the turbulent

dissipation effect is the weakest inside the cavity (Cai et al., 2018b). Therefore, both increasing equivalence ratio and optimizing the ignition site in the cavity are practical ways to ensure a successful ignition process.

Fig. 7 shows a successful cavity ignition process after ignition in the rear of the cavity floor of case 3. The HRR and H_2O distributions in the local cavity region present different variations compared to that of cases 1–2. The initial flame propagates towards the cavity front wall quickly after ignition and forms a large heat release region inside the cavity. After the initial flame propagates out of the cavity from the rear edge, the heat release region inside the cavity decreases gradually. Finally, a large intense heat release region is formed in the cavity shear layer with no heat release region located inside the cavity.

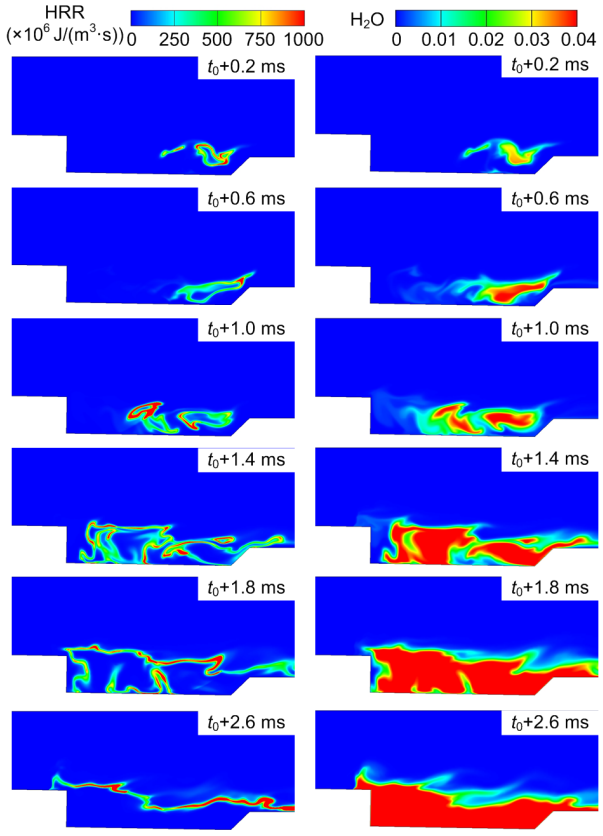

Fig. 7 Successful cavity ignition process after ignition in the rear of the cavity floor (case 3). References to color refer to the online version of this figure

The successful ignition process of case 3 demonstrates that the growing factor has a larger effect than the decaying factor after ignition in the rear of the cavity floor. It is shown that there exists a clockwise direction recirculation flow inside the cavity and the most intense shearing flow is located in the rear cavity. The recirculation flow inside the cavity and the shearing flow can be obtained from both numerical simulation (Cai et al., 2018b) and experimental investigation (Kirik et al., 2014). The shearing flow located in the rear cavity has been shown by Cai et al. (2018b). The shearing flow in the rear cavity has also been investigated by other researchers (Beresh et al., 2016; Zhao et al., 2016). Accordingly, the flame movement speed of case 3 is the biggest, forming the largest heat release region compared to those of cases 1–2 at the same time. Although the turbulent dissipation environment in the rear cavity is also severe, the growing flame supported by consuming fuel consistently along the flame movement routine acts as the dominant effect.

Fig. 8 gives another flame extinguishing process of case 4 after ignition in the rear side of the cavity shear layer. The induced heat release region at 0.2 ms is the smallest compared to those of cases 1–3, and the initial flame only exists a short time before disappearing. Obviously, the decaying factor exerts a dominant effect during all time sequences of case 4, and the flame is seen to be blown off directly in the cavity shear layer due to the high speed of the supersonic core flow. The supersonic core flow in the shear layer has been presented by Cai et al. (2018e) using numerical simulation. They investigated the fuel transport and mixing process in a scramjet combustor. The sonic line can be observed from the shearing flow, and the sonic line in the shearing flow indicates that supersonic flow exists in the shear layer. The supersonic flow in the shear layer can also be observed by Zhao et al. (2016)'s experimental research. Based on the earlier discussion regarding the flame extinguishing mode of cases 1 and 2, the flame extinguishing mechanism of case 4 is seen to be different from the above cases and can be designated as the blown-off extinguishing mode.

The HRR intensity along the ignition process can be calculated according to the HRR spatial integration of the computational domain. As shown in Fig. 9, the quantitative comparison is in accordance with the above qualitative descriptions and presents

more statistical flame behaviors up to 5 ms. We can see that despite case 3, other cases all achieve flame extinguishing state with barely no HRR intensity at the end. Between 0 and 0.5 ms after ignition, it is interesting to note that the HRR intensity of case 3 is less than that of case 1. As reported previously (Cai et al., 2016, 2018b), the turbulent dissipation is the weakest in the cavity angular recirculation zone and it is the strongest in the rear cavity region. After 0.5 ms, the HRR intensity of case 3 continued to increase. Considering the flame movement speed of case 3, the increase in HRR intensity is due to the formation of a larger heat release region by consuming more fuel. Therefore, it can be concluded that both the favorable flow field and the large heat release region are important for the ignition process.

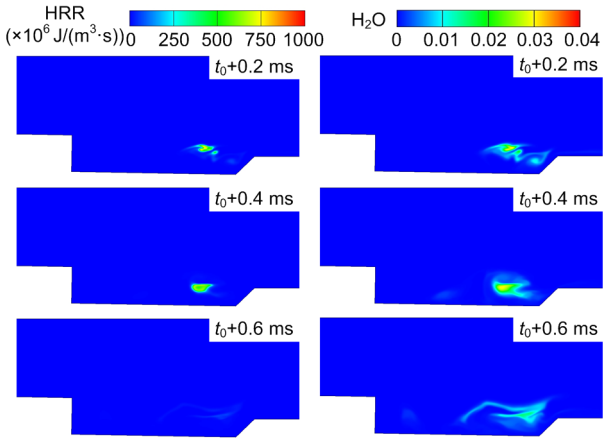

Fig. 8 Blown-off extinguishing mode after ignition in the rear side of the cavity shear layer (case 4). References to color refer to the online version of this figure

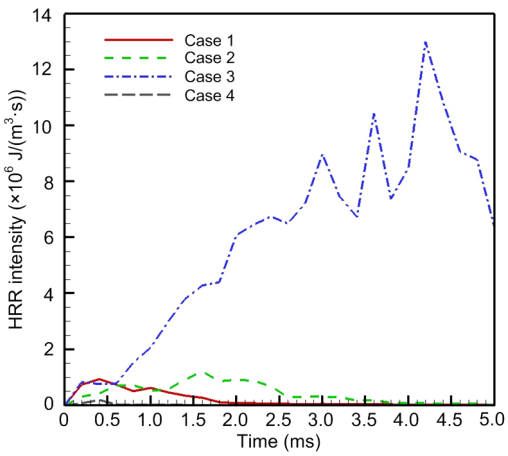

Fig. 9 Comparison of HRR intensities of the supersonic combustor during the ignition process

Despite the HRR and H_2O distributions presented above, the enstrophy distribution as well as the most intense HRR region in the local cavity region of case 3 is given in Fig. 10. Enstrophy (Ω^2, where Ω is the magnitude of the vorticity) can be used to represent the local turbulent flow characteristics since it represents the production of turbulence. The turbulent flow field in the cavity represented by the enstrophy distribution of case 3 is in accordance with previous studies (Cai et al., 2016, 2018b). In Fig. 10, the distributions of HRR and enstrophy were combined in one figure to describe the local turbulent flow characteristics where the HRR appears; the distributions of enstrophy and HRR are shown by two different colorbars. The HRR distribution is shown by the red colorbar. It is seen that there exists obvious enstrophy distributed inside and outside the most intense HRR region during the ignition process, and the chemical reaction also influences the turbulent flow field. Therefore, the growing factor and decaying factor mentioned above can be used to judge the ignition process as a whole. Actually, the ignition process is a complicated interaction between the chemical reaction and the turbulent flow field which should be the subject of further research.

4 Conclusions

In this study, the ignition process in an ethylene-fueled supersonic combustor with a rear-wall-expansion cavity was investigated numerically by a 2D LES method. The ethylene chemical mechanism of 35-step with 20-specie used in this study was validated comprehensively against both experimental data and detailed mechanism through CHEMKIN calculations. The effect of different ignition sites inside the cavity on the ignition process was then studied. It was found that the region in the rear of the cavity floor is an optimized ignition site with a favorable flow field environment and initial flame movement routine. According to the different ignition behaviors after ignition at different sites, two extinguishing modes could be identified: blown-off extinguishing mode and flow dissipation extinguishing

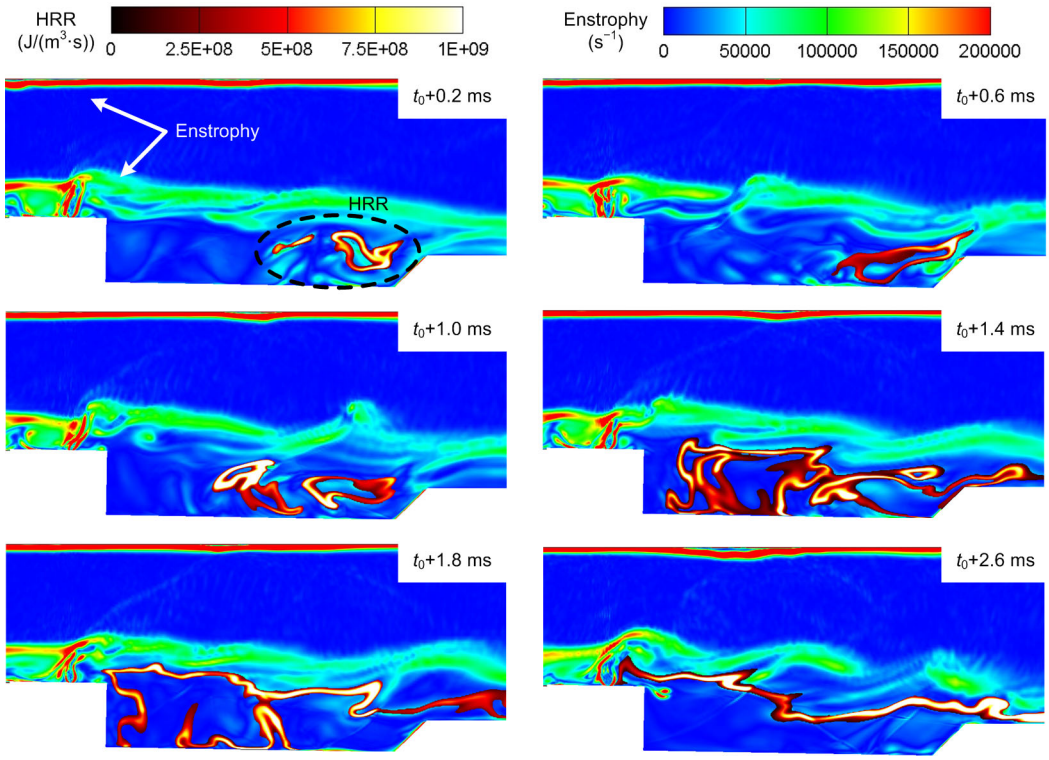

Fig. 10 Enstrophy distribution together with the most intense HRR distribution in the local cavity region of case 3. References to color refer to the online version of this figure

mode. Blown-off extinguishing mode mainly occurs after ignition near the cavity shear layer, in which the flame kernel will be blown off directly due to the high speed of the supersonic core flow. The flow dissipation extinguishing mode is likely to occur after ignition near the front and middle cavity floor as a result of the flow stream evolution and limited chemical reactions. Despite the discussion on turbulent flow field affecting the chemical reaction, it is also demonstrated that the chemical reaction itself affects the turbulent flow field. In short, the initial flame movement routine is an important issue during the ignition process, including both moving towards a favorable flow field and forming a large heat release region. To ensure a successful ignition process, it is indicated that both increasing equivalence ratio and optimizing the ignition site in the cavity are practical routes.

Contributors

Zun CAI and Yong-chao SUN designed the research. Yong-chao SUN and Zun CAI processed the corresponding data and wrote the first draft of the manuscript. Tai-yu WANG and Ming-bo SUN helped to organize the manuscript. Cheng GONG and Yu-hui HUANG revised and edited the final version.

Conflict of interest

Yong-chao SUN, Zun CAI, Tai-yu WANG, Ming-bo SUN, Cheng GONG, and Yu-hui HUANG declare that they have no conflict of interest.

References

Barnes FW, Segal C, 2015. Cavity-based flameholding for chemically-reacting supersonic flow. *Progress in Aerospace Sciences*, 76:24-41. https://doi.org/10.1016/j.paerosci.2015.04.002

Baurle RA, Mathur T, Gruber MR, et al., 1998. A numerical and experimental investigation of a scramjet combustor for hypersonic missile applications. Proceedings of the 34th AIAA/ASME/SAE/ASEE Joint Propulsion Conference and Exhibit. https://doi.org/10.2514/6.1998-3121

Ben-Yakar A, Hanson RK, 2001. Cavity flame-holders for ignition and flame stabilization in scramjets: an overview. *Journal of Propulsion and Power*, 17(4):869-877. https://doi.org/10.2514/2.5818

Beresh SJ, Wagner JL, Casper KM, 2016. Compressibility effects in the shear layer over a rectangular cavity.

Journal of Fluid Mechanics, 808:116-152. https://doi.org/10.1017/jfm.2016.540

Cai Z, Liu X, Gong C, et al., 2016. Large eddy simulation of the fuel transport and mixing process in a scramjet combustor with rearwall-expansion cavity. *Acta Astronautica*, 126:375-381. https://doi.org/10.1016/j.actaastro.2016.05.010

Cai Z, Wang ZG, Sun MB, et al., 2017. Large eddy simulation of the flame propagation process in an ethylene fueled scramjet combustor in a supersonic flow. Proceedings of the 21st AIAA International Space Planes and Hypersonics Technologies Conference, p.2017-2148. https://doi.org/10.2514/6.2017-2148

Cai Z, Zhu JJ, Sun MB, et al., 2018a. Effect of cavity fueling schemes on the laser-induced plasma ignition process in a scramjet combustor. *Aerospace Science and Technology*, 78:197-204. https://doi.org/10.1016/j.ast.2018.04.016

Cai Z, Sun MB, Wang ZG, et al., 2018b. Effect of cavity geometry on fuel transport and mixing processes in a scramjet combustor. *Aerospace Science and Technology*, 80:309-314. https://doi.org/10.1016/j.ast.2018.07.028

Cai Z, Zhu JJ, Sun MB, et al., 2018c. Ignition processes and modes excited by laser-induced plasma in a cavity-based supersonic combustor. *Applied Energy*, 228:1777-1782. https://doi.org/10.1016/j.apenergy.2018.07.079

Cai Z, Sun M, Wang Z, 2018d. Large eddy simulation of the flow structures and mixing fields in a rear-wall-expansion cavity. Proceedings of the 9th Asian Joint Conference on Propulsion and Power, AJCPP2018-091.

Cai Z, Zhu JJ, Sun MB, et al., 2018e. Spark-enhanced ignition and flame stabilization in an ethylene-fueled scramjet combustor with a rear-wall-expansion geometry. *Experimental Thermal and Fluid Science*, 92:306-313. https://doi.org/10.1016/j.expthermflusci.2017.12.007

Chang JT, Zhang JL, Bao W, et al., 2018. Research progress on strut-equipped supersonic combustors for scramjet application. *Progress in Aerospace Sciences*, 103:1-30. https://doi.org/10.1016/j.paerosci.2018.10.002

Curran ET, 2001. Scramjet engines: the first forty years. *Journal of Propulsion and Power*, 17(6):1138-1148. https://doi.org/10.2514/2.5875

Dong G, Fan BC, Ye JF, 2008. Numerical investigation of ethylene flame bubble instability induced by shock waves. *Shock Waves*, 17(6):409-419. https://doi.org/10.1007/s00193-008-0124-3

Egolfopoulos FN, Law CK, 1991. An experimental and computational study of the burning rates of ultra-lean to moderately-rich $H_2/O_2/N_2$ laminar flames with pressure variations. *Symposium (International) on Combustion*, 23(1):333-340. https://doi.org/10.1016/S0082-0784(06)80276-6

Hassan MI, Aung KT, Kwon OC, et al., 1998. Properties of laminar premixed hydrocarbon/air flames at various pressures. *Journal of Propulsion and Power*, 14(4):479-488. https://doi.org/10.2514/2.5304

Huang W, Yan L, 2013. Progress in research on mixing techniques for transverse injection flow fields in supersonic crossflows. *Journal of Zhejiang University-SCIENCE A (Applied Physics & Engineering)*, 14(8):554-564. https://doi.org/10.1631/jzus.A1300096

Huang W, Liu J, Yan L, et al., 2013. Multiobjective design optimization of the performance for the cavity flameholder in supersonic flows. *Aerospace Science and Technology*, 30(1):246-254. https://doi.org/10.1016/j.ast.2013.08.009

Huang W, Li MH, Ding F, et al., 2016. Supersonic mixing augmentation mechanism induced by a wall-mounted cavity configuration. *Journal of Zhejiang University-SCIENCE A (Applied Physics & Engineering)*, 17(1):45-53. https://doi.org/10.1631/jzus.A1500244

Jomaas G, Zheng XL, Zhu DL, et al., 2005. Experimental determination of counterflow ignition temperatures and laminar flame speeds of C_2–C_3 hydrocarbons at atmospheric and elevated pressures. *Proceedings of the Combustion Institute*, 30(1):193-200. https://doi.org/10.1016/j.proci.2004.08.228

Kirik JW, Goyne CP, Peltier SJ, et al., 2014. Velocimetry measurements of a scramjet cavity flameholder with inlet distortion. *Journal of Propulsion and Power*, 30(6):1568-1576. https://doi.org/10.2514/1.B35195

Kumar K, Mittal G, Sung CJ, et al., 2008. An experimental investigation of ethylene/O_2/diluent mixtures: laminar flame speeds with preheat and ignition delays at high pressures. *Combustion and Flame*, 153(3):343-354. https://doi.org/10.1016/j.combustflame.2007.11.012

Li J, Ma FH, Yang V, et al., 2007. A comprehensive study of ignition transient in an ethylene-fueled scramjet combustor. Proceedings of the 43rd AIAA/ASME/SAE/ASEE Joint Propulsion Conference & Exhibit. https://doi.org/10.2514/6.2007-5025

Li J, Zhang LW, Choi JY, et al., 2015. Ignition transients in a scramjet engine with air throttling part II: reacting flow. *Journal of Propulsion and Power*, 31(1):79-88. https://doi.org/10.2514/1.B35269

Liu X, Cai Z, Tong YH, et al., 2017. Investigation of transient ignition process in a cavity based scramjet combustor using combined ethylene injectors. *Acta Astronautica*, 137:1-7. https://doi.org/10.1016/j.actaastro.2017.04.007

Lv Z, Xia ZX, Liu B, et al., 2017. Preliminary experimental study on solid-fuel rocket scramjet combustor. *Journal of Zhejiang University-SCIENCE A (Applied Physics & Engineering)*, 18(2):106-112. https://doi.org/10.1631/jzus.A1600489

Mathur T, Gruber M, Jackson K, et al., 2001. Supersonic combustion experiments with a cavity-based fuel injector. *Journal of Propulsion and Power*, 17(6):1305-1312.

https://doi.org/10.2514/2.5879

Potturi AS, Edwards JR, 2015. Large-eddy/Reynolds-averaged Navier–Stokes simulation of cavity-stabilized ethylene combustion. *Combustion and Flame*, 162(4):1176-1192. https://doi.org/10.1016/j.combustflame.2014.10.011

Sun MB, Gong C, Zhang SP, et al., 2012. Spark ignition process in a scramjet combustor fueled by hydrogen and equipped with multi-cavities at Mach 4 flight condition. *Experimental Thermal and Fluid Science*, 43:90-96. https://doi.org/10.1016/j.expthermflusci.2012.03.028

Wang H, You XQ, Joshi AV, et al., 2007. USC Mech Version II. High-temperature Combustion Reaction Model of H_2/CO/C1-C4 Compounds. University of Southern California, USA. http://ignis.usc.edu/USC_Mech_II.htm

Wang X, Zhong FQ, Gu HB, et al., 2015. Numerical study of combustion and convective heat transfer of a Mach 2.5 supersonic combustor. *Applied Thermal Engineering*, 89:883-896. https://doi.org/10.1016/j.applthermaleng.2015.06.071

Wang ZG, Wang HB, Sun MB, 2014. Review of cavity-stabilized combustion for scramjet applications. *Proceedings of the Institution of Mechanical Engineers, Part G: Journal of Aerospace Engineering*, 228(14):2718-2735. https://doi.org/10.1177/0954410014521172

Wang ZG, Cai Z, Sun MB, et al., 2016. Large eddy simulation of the flame stabilization process in a scramjet combustor with rearwall-expansion cavity. *International Journal of Hydrogen Energy*, 41(42):19278-19288. https://doi.org/10.1016/j.ijhydene.2016.09.012

Yang V, Li J, Choi JY, et al., 2010. Ignition transient in an ethylene fueled scramjet engine with air throttling part II: ignition and flame development. Proceedings of the 48th AIAA Aerospace Sciences Meeting Including the New Horizons Forum and Aerospace Exposition. https://doi.org/10.2514/6.2010-410

Zhao Y, Liang J, Zhao Y, 2016. Non-reacting flow visualization of supersonic combustor based on cavity and cavity–strut flameholder. *Acta Astronautica*, 121:282-291. https://doi.org/10.1016/j.actaastro.2015.12.040

中文概要

题　目：超声速燃烧室内凹腔点火过程的数值研究

目　的：超燃冲压发动机的点火过程是超声速燃烧领域的重要课题之一。目前，针对超燃冲压发动机燃烧室点火过程的研究以实验研究为主，数值研究则相对较少。本文旨在基于大涡模拟研究点火位置对点火过程的影响，并在此基础上分析导致点火失败的原因。

创新点：1. 基于大涡模拟，研究点火位置对点火过程建立的影响；2. 发现了流动耗散和直接吹熄两种熄火模式。

方　法：1. 基于 CHEMKIN，选择合适的化学反应机理；2. 在简化化学反应机理的基础上，利用大涡模拟研究不同点火位置对点火过程的影响；3. 分析数值仿真数据，寻找能成功实现点火的点火位置，并探讨导致点火失败的因素。

结　论：1. 在凹腔后缘处点火可以成功实现发动机点火；2. 发现了两种点火失败的模式，即流动耗散模式和直接吹熄模式；3. 流动耗散模式主要发生在凹腔前缘和凹腔中部，而直接吹熄模式主要发生在剪切层中。

关键词：点火过程；凹腔；超声速燃烧室；数值模拟